Advances in Science and Technology Research Journal, 2026, 20(1), 152–161 https://doi.org/10.12913/22998624/210473 ISSN 2299-8624, License CC-BY 4.0

Received: 2025.07.26 Accepted: 2025.09.08 Published: 2025.11.21

Application of anion exchange membranes Fumasep FAA-3-PK-130 and PiperION as components of a laboratory electrolyzer for electrochemical hydrogen evolution

Aleksandra J. Domańska¹, Piotr Maciej Skitał^{2*}

- ¹ Doctoral School of the Rzeszow University of Technology, 35-959 Rzeszów, Poland
- ² Faculty of Chemistry, Rzeszow University of Technology, 35-959 Rzeszów, Poland
- * Corresponding author's e-mail: pskital@prz.edu.pl

ABSTRACT

The aim of this study was to investigate the performance of anion exchange membranes in the electrochemical hydrogen evolution process, which is an important issue in the context of the development of sustainable hydrogen technologies. Fumasep FAA-3-PK-130 and PiperION membranes (40 µm) were used, their properties enabling operation in 1 M NaOH solution at room temperature. The cathodes employed were 304 stainless steel and a nanostructured Co-Ni alloy coating obtained by cobalt and nickel co-deposition. The nanostructured coating enabled resistance reductions of 25.50% and 36.61% for FAA-3-PK-130 and PiperION, respectively. Comparative analysis showed that PiperION exhibited lower resistance but also lower conductivity than FAA-3. Membrane thicknesses were examined after activation to the OH⁻ form. PiperION demonstrated higher liquid absorption, with a swelling ratio of 42.50%, compared to 32.31% for FAA-3. Owing to its advanced polymer backbone, PiperION offers lower resistance and improved anion transport selectivity, while maintaining high stability in alkaline environments. These studies allowed us to evaluate the properties of modern AEM membranes under alkaline conditions and compare their potential for use in hydrogen electrolysis.

Keywords: anion exchange membrane, electrolytic hydrogen production, hydrogen efficiency, alkaline water electrolysis.

INTRODUCTION

Hydrogen production by electrolysis powered by renewable energy sources (RES) is an environmentally friendly method of obtaining hydrogen. The resulting hydrogen can be used to generate clean energy [1]. However, global hydrogen production still relies heavily on carbon-based feedstocks [2]. In a report published in 2024, the International Energy Agency (IEA) noted that only 1 Mt of low-emission hydrogen was produced in 2023, of which merely 0.1 Mt originated from electrolysis [3]. The high cost of this method contributes to the low share of green hydrogen in overall production and limits its large-scale industrial deployment [4].

Water electrolysis requires the use of a strong electrolyte, either acidic or alkaline, to ensure

efficient and continuous charge transport between electrodes [5]. Another important component in the electrolyzer setup is the ion-exchange membrane, composed of functional ionic groups attached to a polymer backbone [6]. When the membrane conducts protons (H⁺), the process is referred to as PEM (proton exchange membrane) electrolysis. In contrast, membranes that allow hydroxide ions (OH⁻) to pass are used in AEM (anion exchange membrane) electrolysis [7]. PEM electrolysis enables higher current densities and thus greater efficiency. However, commercially available proton-exchange membranes such as Nafion are expensive. Moreover, the use of noble metals such as platinum, iridium, and ruthenium as catalysts at the cathode and anode further increases costs, due to the strongly acidic environment of the membrane [8, 9]. Alkaline electrolysis allows for the use of more affordable transition metal catalysts, such as nickel and cobalt [10]. As shown in studies [11, 12], AEM electrolysis can deliver comparable performance while significantly reducing costs, making it a cost-effective alternative [13]. Nevertheless, AEM technology still requires further investigation regarding membrane and catalyst stability, as well as energy efficiency, to increase hydrogen's role in the future energy economy [14, 15].

There are many ion-exchange membranes available on the market. Typically, anion-exchange membranes are constructed of a hydrocarbon backbone with quaternary ammonium groups, which bind water and allow the transport of OH- ions [16]. As indicated by Wijaya et al. [17] Fumasep® FAA-3 series produced by Fumatech are materials that provide performance, durability, versatility of applications and at the same time affordability. The series includes products with different thicknesses but also reinforced options [18]. The Fumasep FAA-3-PK-130 membrane was described by Giovanelli et al. [19], as reported by the authors contains FAA-3 as an ionomer with poly (phenylene oxide) (PPO) as the backbone and polyetheretherketone (PEEK) as the auxiliary polymer matrix. This makes it possible to improve the mechanical properties while mitigating the swelling effect during water adsorption. Due to its high ionic conductivity, durability and favourable cost/efficiency ratio, the Fumasep FAA-3-PK-130 membrane is a benchmark in the evaluation of newly developed anion exchange membranes.

Another example of ion exchange membranes is the PiperION® offered by VersogenTM, produced from a functional poly(arylpiperidine) resin. Based on a study by Hyun et al. [20] showed that the PiperION membrane did not show any damage compared to FAA-3, among others. Furthermore, it had better stability due to its higher boundary stress. A variant with microporous poly(tetrafluoroethylene) (PTFE) reinforcement is also available [21]. The manufacturer indicates that the lack of reinforcement allows a higher ionic conductivity, while the mechanical reinforcement of the membrane provides a higher performance. Rutjens et al. studied the effect of PiperION thickness on CO, electroreduction performance. They showed that membranes with thicknesses of 22 and 35 µm provided better performance. In contrast, a membrane

with a thickness of 80 μm introduced a higher internal resistance and resulted in significantly higher cell voltages [22].

The present work deals with the use of commercially available anion exchange membranes and comparisons of their performance in the electrolytic hydrogen evolution process. The electrolyser design used a Fumasep FAA-3-PK-130 membrane and a PiperION® self-supporting membrane (without reinforcement) with a thickness of 40 µm. The role of the cathode was played by 304 steel and a Co-Ni alloy coating, which was obtained by electrodeposition on the surface of 304 steel. By measuring the potential of the electrode system and the voltage of the system as a function of current, the influence of the membrane as an electrolyser element was observed. These results were compared with measurements recorded without membranes, which were published in an earlier paper [23]. The conducted research aims to supplement the current knowledge on the practical application of modern AEM membranes available on the market and to indicate directions for their further optimization in the alkaline electrolysis process as an ecological hydrogen production.

MATERIALS AND METHODS

Preparation of membranes

The membranes were purchased from Fuel Cell Store and were supplied in dry form, Table 1 contains their parameters and properties. As recommended by the manufacturers, the membranes were converted to OH⁻ form by placing them in NaOH solutions. The FAA-3-PK-130 membrane was placed for 24 h in 0.5 M NaOH (p.a., CHEMPUR) at room temperature. The PiperION, on the other hand, was placed in the same conditions and concentration for one hour, after which the solution was replaced with fresh solution and left for another hour, as recommended by the manufacturer. After rinsing with distilled water, the membranes were ready for the electrolysis process.

The amount of phenyl groups and the presence of ether bridges in the polymer backbone determine the susceptibility of the membrane to oxidation. Based on the available literature [19, 24], it can be concluded that FAA-3-PK-130, which contains numerous phenyl groups linked

Table 1. AEM parameters provided by producer	Table 1. AEM	parameters	provided	by	producers
---	--------------	------------	----------	----	-----------

Parameter	AEM			
Parameter	FAA-3-PK	PiperION		
Nominal thickness [µm]	130	40		
Type of functional group	Quaternary ammonium groups	Piperazine groups		
Amount of phenyl groups	Very large	Lower concentration		
Presence of ether bridges	Yes	None		
Range of stability (pH) w 25 °C	0–14	1–14		

by ether bridges, is more susceptible to oxidative degradation than PiperION, whose aromatic structure is devoid of such bonds, resulting in higher chemical stability.

Using the Digital Thickness Gauge produced by Mitutoyo (Japan), membrane thicknesses were measured as OH^- by taking measurements on the measured area, then the arithmetic mean was calculated and the standard deviation (\pm SD) was reported.

Electrolytic hydrogen evolution

The designed and constructed set-up of the laboratory electrolyser, which allows simultaneous collection of hydrogen and oxygen. The laboratory electrolyser was made of glass, hence the need to use NaOH solution instead of potassium hydroxide. The upper part of the chambers contained a glass drain, which was connected via rubber hoses to the gas collection system and sintered to the electrolytic key. The gas collection system was filled with water, which was displaced by hydrogen and oxygen, respectively, during the measurement. The electrolytic key used 0.6 M Na₂SO₄, in which the reference electrode, a calomel electrode, was also immersed. This arrangement was used in earlier work [23]. Hydrogen electrolysis was carried out in 1 M NaOH. A 304 steel sheet acted as the anode, while 304 steel and a 5 µm thick Co-Ni alloy coating were also used as the cathode. To ensure the tightness of the system, silicone gaskets with clamps were used, while the sinters connecting the electrolytic keys to the cell assembly were protected with silicone grease.

The research methodology consisted of establishing a constant current on the power supply and recording the potentials of the cathode $E_{\rm c}$ and anode $E_{\rm a}$. The volume of gases produced was also measured. From these measurements, the efficiencies of the electrolysis process were calculated.

RESULTS AND DISCUSSION

Efficiency of the laboratory electrolyser

During the measurement, the volumes of hydrogen and oxygen produced were measured at a constant current, and the dependence of the total volume of the collected gases produced in one hour was determined, as shown in Figure 1. On the basis of the determined regression and the value of the parameter R², it was determined that this dependence was linear. During the calculation, it is the potential of the cathode and anode that verifies how the component affects the efficiency of the electrolysis process.

A parameter that significantly affects the maximum current density is the distance between the cathode and anode, which is confirmed by the work of [25, 26]. Yuzer et al. [27] investigated the effect of reducing the distance between the electrodes from 2.2 cm to 0.8 cm in the electrolysis process. They showed that the energy yield increased by 34%, the hydrogen production rate by 47% and the current density values by about 42%. Figure 2 shows the effect of the inter-electrode distance at maximum current density in the laboratory electrolyser. Analysis of the voltages recorded at 100 mA/cm² allows us to conclude that a six-fold (by 2.5 cm) reduction in distance allowed the system voltage to be reduced by two times under these current conditions.

Hydrogen evolution at constant current values

Hydrogen evolution in alkaline solution was carried out using the aforementioned materials as membranes. By setting a constant current value, the response of the system was recorded in the form of the total voltage, as well as the cathode and anode potential. On this basis, U(j) relationships were plotted, as represented in Figure 3, for the 304 steel cathode (A) and alloy coating (B) measurements.

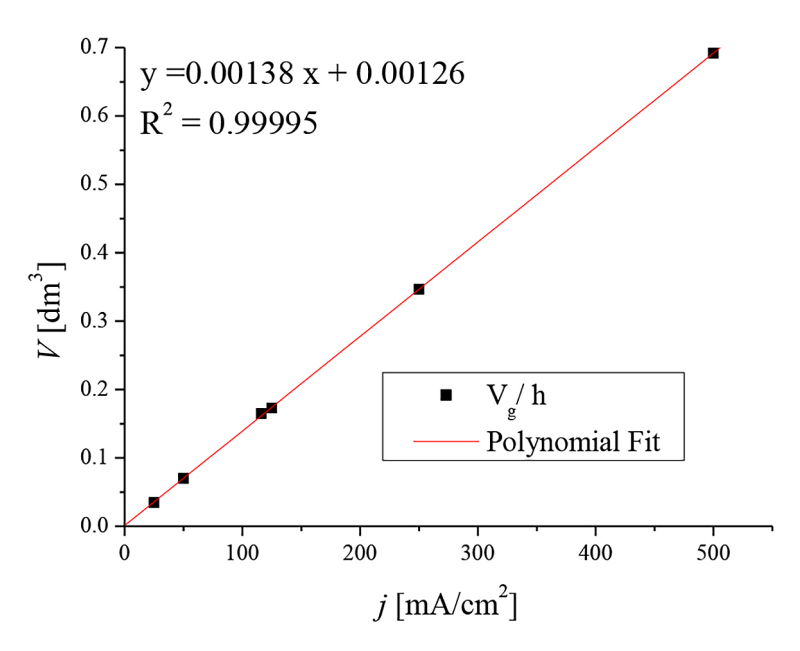


Figure 1. Dependence of the total volume of gases collected on the current density produced in one hour

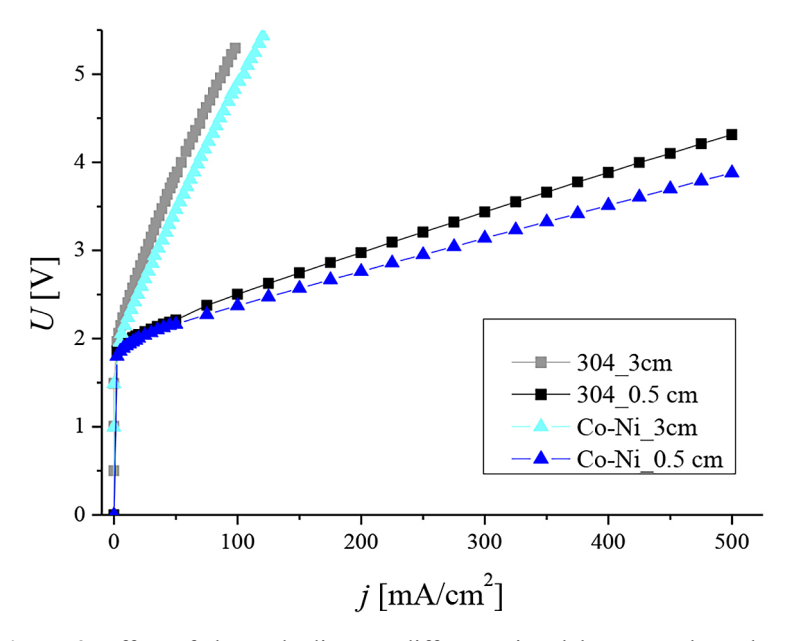


Figure 2. Effect of electrode distance difference in a laboratory electrolyser

Based on the measurements, the PiperION membrane, compared to FAA-3-PK-130, introduces less internal resistance in the electrolyser system, as it exhibits lower voltages at a given current value. The Co-Ni alloy coating nanostructure performs better as a cathode than chromium-nickel steel, in both cases, without and with membranes.

The potential distribution is shown in Figure 4, with graph (A) showing the data for the chromonickel cathode and (B) for the cobalt-nickel coated cathode. The greatest differences were

observed in the potential characteristics of the anode, where the substrate of the electrode reaction is OH-, an anion passed through the membranes. The cathode in anion-exchange membrane systems plays a key role in determining overall cell performance, stability and efficiency [28]. The cathodes we used were electropolished (smooth) chromonickel and a Co-Ni alloy nanostructure, characterised by higher roughness. The porosity and hydrophobicity of the cathode affect water distribution, with optimally loaded cathodes supporting better water management and reducing

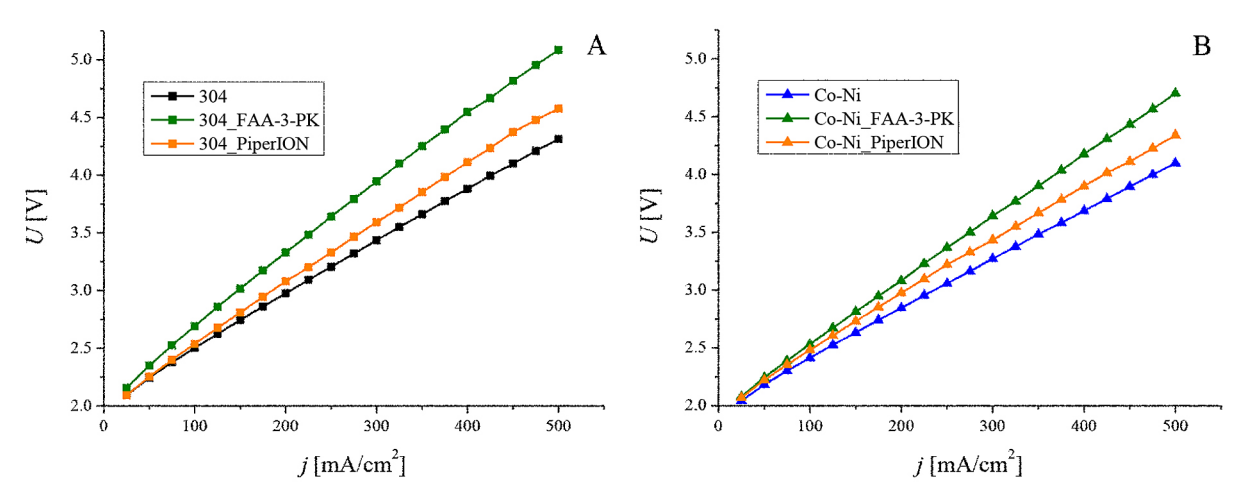


Figure 3. Dependence of electrolyser voltage as a function of current density for the system without membrane, with FAA-3-PK membrane and PiperION for 304 steel cathode (A) and Co-Ni alloy coating (B)

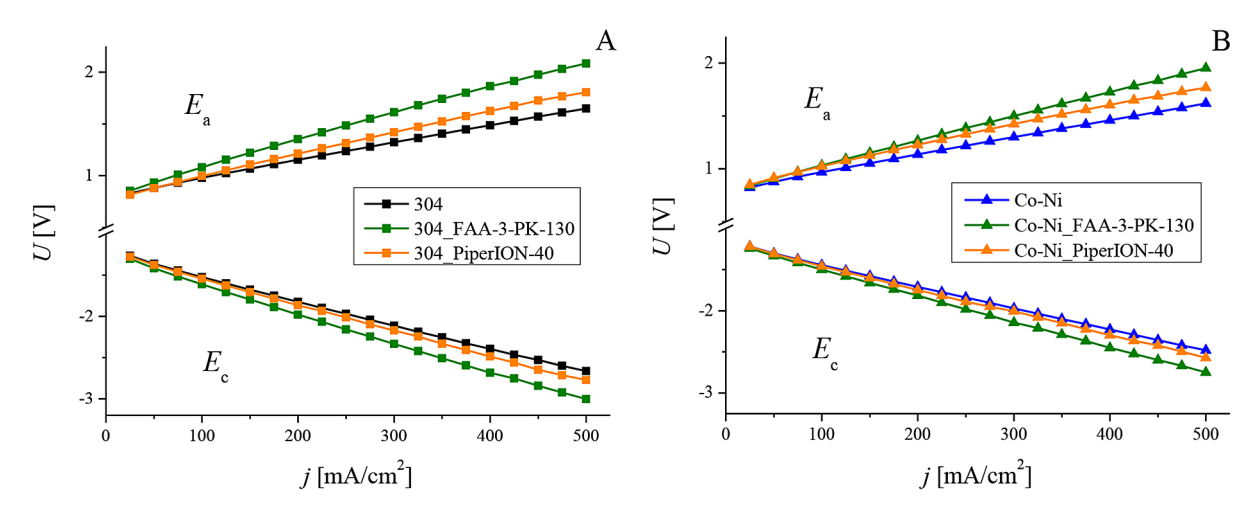


Figure 4. Potentials of cathode E_c and anode E_a as a function of current for (A) – 304 steel and (B) – Co-Ni nanostructure

mass transport losses on the cathode, which indirectly supports anode performance [29]. The studies of Li et al. [30] and Faid et al. [31] indicates that electrochemical oxidation of phenyl groups, located in the membrane, under the influence of OER potentials, can lead to a decrease in local pH, which subsequently reduces catalytic activity. This means that the chromonickel used as anode should be replaced with a more active material, especially when anion exchange membranes are used in the system.

The membranes used in the study differ in material, structure but also in thickness. Hence, the question is whether PiperION, despite its material, would not show inferior properties in terms of performance if its thickness were similar to FAA-3-PK. According to a study by Kong et al. [32], the 80 µm PiperION showed

a surface resistance of $0.344~\Omega cm^2$, while the $50~\mu m$ thick FAA-3 showed a surface resistance of $0.4~\Omega cm^2$. The authors indicate that the electrolysis performance is significantly dependent on the surface resistance of the membranes. From this, we can concludeww that thickness has a significant effect on a membrane of the same type [33], and that it is the material and its properties, such as ion exchange capacity or surface resistivity (as well as volume resistivity), that determine the membrane performance in hydrogen evolution.

Based on the plotting of the U(I) relationship and linear regression, the average resistance R was determined as the slope coefficient of the straight line, as shown in Figure 5. The resistance of the set using membranes was then compared with the resistance characterising the set without the additional element, the difference representing the contribution of the membrane to the total resistance.

When using 304 steel as the cathode for the FAA-3-PK-130 and PiperION-40 membrane, average resistances of 0.758 and 0.306 Ω were determined, respectively, while 0.604 and 0.224 Ω were determined for the Co-Ni coating. The nanostructure of the alloy coating resulted in lower resistances of 25.50 % and 36.61 % for FAA-3-PK-130 and PiperION-40, respectively. These results confirm the important role played by the cathode material in electrolysis with anion-exchange membranes.

The system we present here involves a membrane that is in the field region parallel between the electrodes while not adjacent to them, so the Through-Plane (TP) method, which takes into account the direction of the current through the thickness of the membrane, was used to determine the ionic conductivity σ [34]. The value of σ [mS/cm] can be calculated from Equation 1 given in the paper [35]:

$$\sigma = \frac{l}{A \cdot R} \tag{1}$$

where: l – membrane thickness [cm], R – measured resistance [Ω], A – contact area of measuring electrodes [cm²].

The surface resistance ASR [Ω cm²], defined as the product of membrane area and its resistance, was also taken into account [36], as shown in Equation 2:

$$\sigma = \frac{l}{ASR} \tag{2}$$

The active area refers to the part of the membrane through which current flows, i.e., the cross-sectional area between the electrodes. Assuming that the current flows through an area equal to the surface of the cathode facing the membrane (as it limits the cross-sectional area of current flow), the surface resistance (ASR) value in this case is equal to the measured resistance R. Based on the ASR values, the ionic conductivity σ was calculated. Somayyed et al. [37], in their calculations involving the FAA-3-PK-130 membrane, used the area of the membrane immersed in the electrolyte, which does not necessarily match the electrode surface. Considering the membrane area between the seals (in contact with the electrolyte), the value amounts to 5.3025 cm². Numerical results are presented in Table 2. The values vary depending on the adopted assumptions, highlighting the importance of evaluating not only experimental parameters and conditions but also calculation methods and underlying assumptions.

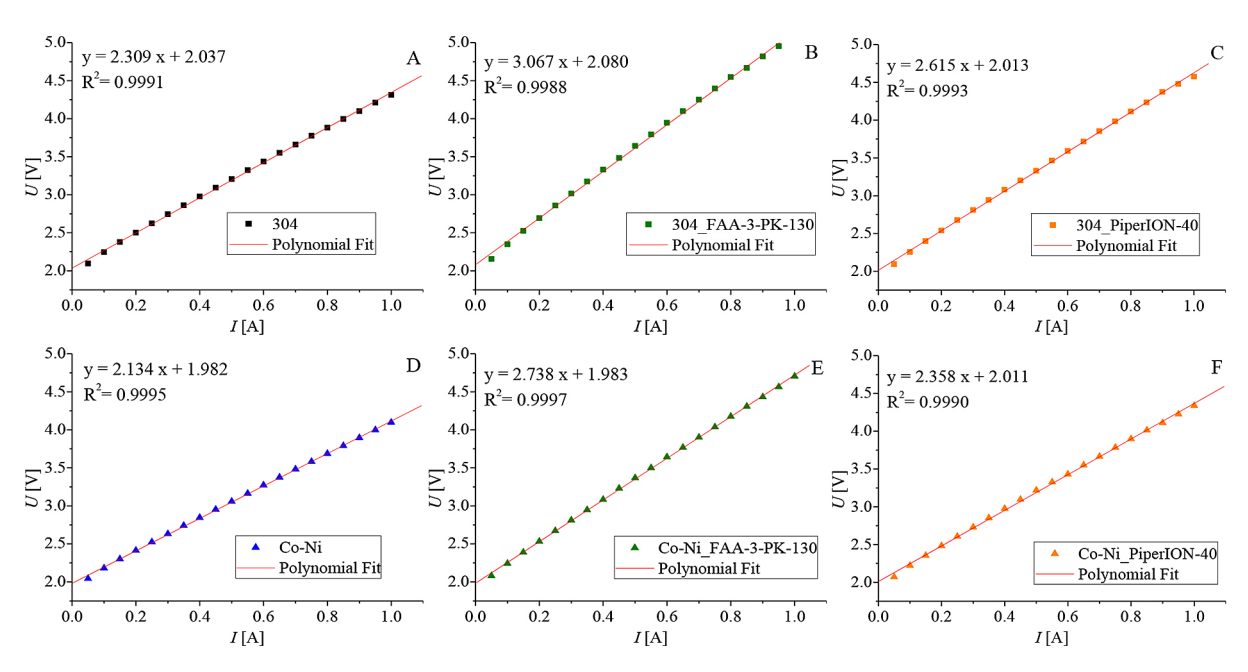


Figure 5. Dependence of system voltage as a function of current with linear regression for (A, B, C) – 304 steel and (D, E, F) – Co-Ni nanostructure. The results shown as (A, D) represent measurements without the use of membranes, while (B, E) and (C, F) are results recorded with the FAA-3-PK-130 and PiperION-40 membranes, respectively

Literature sources also provide information on the method for determining the "true hydroxide conductivity", which takes into account the membrane thickness after activation, i.e., after swelling [18]. The thickness was measured using a micrometer, with average values of 0.172 ± 0.003 mm and 0.057 ± 0.002 mm for FAA and PiperION, respectively. Based on these measurements, the membrane swelling ratio $SR_{\%}$ was calculated using Equation 3, where the subscripts w and d refer to the membrane in the wet and dry states, respectively. The $SR_{\%}$ values indicate that the membranes increased their thickness by 32.31% and 42.50%, with PiperION showing a greater liquid uptake capacity.

$$SR_{\%} = \frac{l_w - l_d}{l_d} \cdot 100\%$$
 (3)

(3A comparative analysis of the two membranes tested indicated that PiperION has lower resistance, but also conductivity. This phenomenon is explained by Luo et al. [38], indicating a more amorphous microstructure in the case of PiperION. There are quaternary ammonium groups on the rigid backbone of its polymer. This reduces the dissimilarity between the backbone and the ionic groups. In contrast, FAA-3 has a

less rigid backbone because it contains ether groups. In general, conductivity increases with water uptake. On the other hand, according to the information found in the paper [39], an increase in water uptake can counteract the conductivity of the material by decreasing the concentration of mobile ions in the hydrophilic phase.

The resistances discussed above refer to average values calculated over a wide current range (0.05–1 A). The difference in voltage at individual measurement points relative to the data recorded without the membrane shows the contribution of the membrane to the lowering of the electrolyser system potential at a given current value. From these results, shown in Figure 6, it is noted that the operation of the PiperION membrane is less dependent on the cathode material than that of the FAA-3-PK, which may be due to its better stability [20].

Influence of membranes on hydrogen evolution efficiency

Measuring the volume of gases produced during alkaline electrolysis allowed the performance of the process with anion exchange membranes to be presented and compared with electrolysis without

Cathode material	304		Co-Ni		Based on the equation	
	FAA-3-PK-130	PiperION-40	FAA-3-PK-130	PiperION-40	reported in the literature	
$ASR [\Omega cm^2] (=R)$	0.758	0.306	0.604	0.224	[34]	
σ [mS/cm]	17.15	13.07	21.52	17.86	[36]	
	3.234	2.465	4.059	3.374	[37]	

Table 2. Calculated values for the average resistance *R* and the surface resistance *ASR* of the membranes

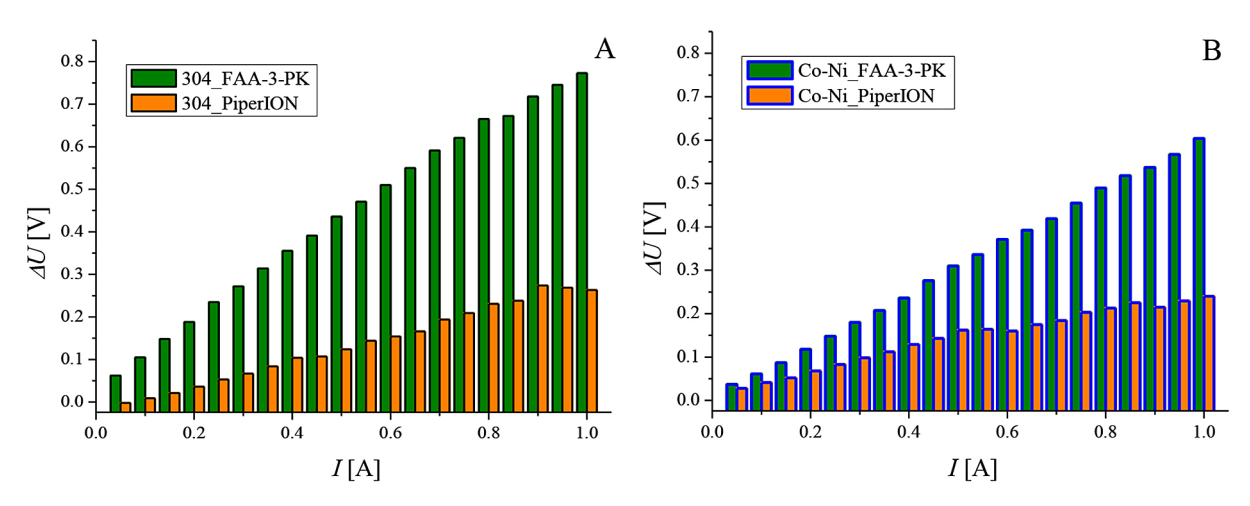


Figure 6. Point voltage difference as a function of current relative to data recorded without the membrane for (A) - 304 steel and (B) - Co-Ni nanostructure

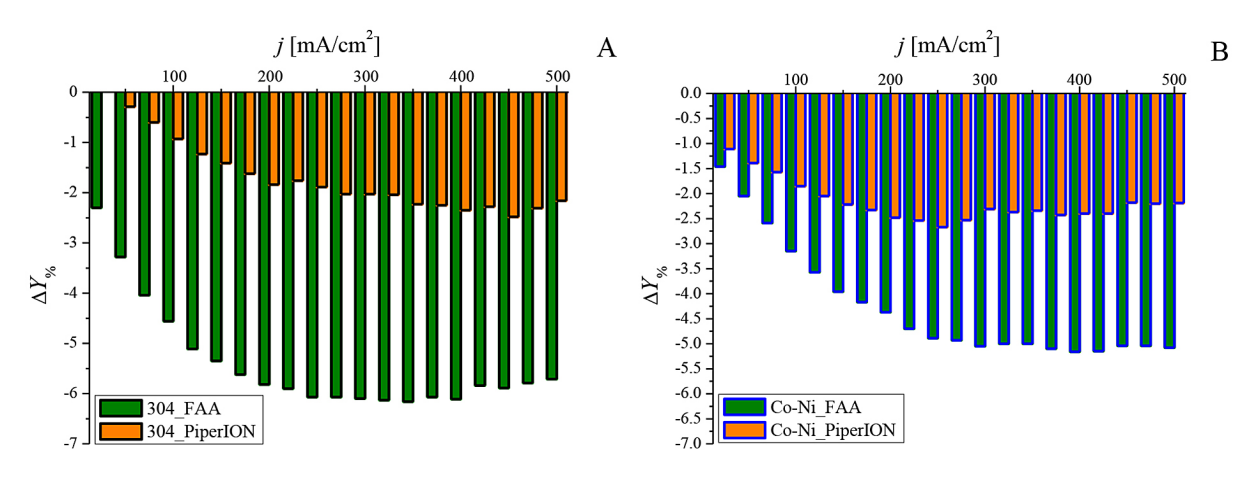


Figure 7. Decrease in percentage yield $Y_{\%}$ of the electrolysis process relative to measurements carried out without AEM for (A) – 304 steel and (B) – Co-Ni nanostructure

Table 5. Try drogon evolution yield parameters measured at a current density of 250 mm em									
Cathode material	304			Co-Ni					
Parameter	Without membrane	FAA-3-PK-130	PiperION-40	Without membrane	FAA-3-PK-130	PiperION-40			
Y _%	50.66	44.60	48.78	55.05	50.16	52.38			
gH ₂ /kWh	12.87	11.32	12.39	13.98	12.69	13.28			
kJ/molH。	564.8	641.6	586.6	519.8	573.1	547.4			

Table 3. Hydrogen evolution yield parameters measured at a current density of 250 mA/cm²

their membranes. Figure 7 shows the decrease in the percentage yield $Y_{\%}$ of the electrolysis process relative to measurements carried out without the use of AEM. The largest difference in membrane performance was registered for the 304 surface, the Co-Ni nanostructure stabilises the hydrogen evolution reaction (HER), and the PiperION membrane causes a smaller decrease in performance. The PiperION membrane showed a smaller drop in efficiency compared to the Co-Ni cathode, but at very low current densities, values which are not considered in industrial electrolysers. Table 3 represents the characteristic parameters for determining the hydrogen evolution efficiency calculated from measurements at a current density of 250 mA/cm².

CONCLUSIONS

- The introduction of an additional membrane element into the system resulted in an increase in resistance and a concomitant increase in electrolyser system voltage. However, this element provides less permeation and mixing of gases (H₂, O₂), which can affect the efficiency of product separation.
- 2. As a classical membrane, FAA-3-PK-130 is a good reference system, but has a higher

- ionic resistance. PiperION, thanks to its modern polymer carrier, offers lower resistance and better selectivity for anion transport, while maintaining high durability in alkaline environments.
- 3. Despite their higher cost, piperazine membranes have greater chemical durability and lower gas permeability, making them an attractive alternative to classical membranes based on quaternary ammonium groups.
- 4. The lower resistance in the AEM leads to a higher yield and improved hydrogen release efficiency. Combined with the enhanced durability and selectivity of modern membranes, this creates promising prospects for the development of next-generation alkaline electrolysers. Future studies could focus on balancing cost, chemical stability and scalability to enable broader industrial implementation.

Acknowledgments

This research was funded by the Minister of Science and Higher Education Republic of Poland within the program "Regional Excellence Initiative" for Rzeszow University of Technology, 2024–2027, agreement no. RID/SP/0032/2024/01.

REFERENCES

- Mazzeo D., Herdem M., Matera N., Wen J. Green hydrogen production: Analysis for different single or combined large-scale photovoltaic and wind renewable systems. Renewable Energy. 2022; 200: 360– 378. https://doi.org/10.1016/j.renene.2022.09.057
- 2. Kumar S., Lim H. An overview of water electrolysis technologies for green hydrogen production. Energy Rep. 2022; 8: 13793–13813. https://doi.org/10.1016/j.egyr.2022.10.127
- 3. IEA. Global Hydrogen Review 2024. IEA, Paris; 2024. https://www.iea.org/reports/global-hydrogen-review-2024
- Badgett A., Ruth M., James B., Pivovar B. Methods identifying cost reduction potential for water electrolysis systems. Curr. Opin. Chem. Eng. 2021; 33: 100714. https://doi.org/10.1016/j.coche.2021.100714
- Domańska A., Skitał P. Mathematical modeling of the hydrogen evolution process on nickel, cobalt, and Co-Ni alloy coatings in acidic and alkaline environments. Chem. Process Eng. NEW. FRONT. 2025; 46(1): e82. https://doi.org/10.24425/ cpe.2025.153667
- 6. Hagesteijn K., Jiang S., Ladewig B. A review of the synthesis and characterization of anion exchange membranes. J. Mater. Sci. 2018; 53: 11131–11150. https://doi.org/10.1007/s10853-018-2409-y
- Carbone A., Campagna Zignani S., Gatto I., Trocino S., Aricò A.S. Assessment of the FAA3-50 polymer electrolyte in combination with a NiMn₂O₄ anode catalyst for anion exchange membrane water electrolysis. Int. J. Hydrogen Energy. 2020; 45(16): 9285–9292. https://doi.org/10.1016/j.ijhydene.2020.01.150
- 8. Serhat Akyüz E., Telli E., Farsak M. Hydrogen generation electrolyzers: Paving the way for sustainable Energy. Int. J. Hydrogen Energy. 2024; 81: 1338–1362. https://doi.org/10.1016/j.ijhydene.2024.07.175
- Campagna Zignani S., Lo Faro M., Carbone A., Italiano C., Trocino S., Monforte G., Aricò A.S. Performance and stability of a critical raw materials-free anion exchange membrane electrolysis cel. Electrochim. Acta. 2022; 413: 140078. https://doi. org/10.1016/j.electacta.2022.140078
- 10. Skitał P., Domańska A. Modeling of the simultaneous hydrogen evolution and cobalt electrodeposition. ChemPhysChem. 2022; 23: e202200148. https://doi.org/10.1002/cphc.202200148
- 11. Bernat R., Milewski J., Dybinski O., Martsinchyk A., Shuhayeu P. Review of AEM electrolysis research from the perspective of developing a reliable model. Energies. 2024; 17(20): 5030. https://doi.org/10.3390/en17205030

- 12. Pandiarajan T., John Berchmans L., Ravichandran S. Fabrication of spinel ferrite based alkaline anion exchange membrane water electrolysers for hydrogen production. RSC Adv. 2015; 5(43): 34100–34108. https://doi.org/10.1039/C5RA01123J
- 13. Chae J.E., Choi J., Lee S., Park C., Kim S. Effects of fabrication parameters of membrane–electrode assembly for high-performance anion exchange membrane fuel cells. J. Ind. Eng. Chem. 2024; 133: 255–262. https://doi.org/10.1016/j.jiec.2023.11.063
- Vincent I., Bessarabov D. Low cost hydrogen production by anion exchange membrane electrolysis: A review. Renewable Sustainable Energy Rev. 2018; 81: 1690–1704. https://doi.org/10.1016/j.rser.2017.05.258
- 15. Zakaria, Z. and Kamarudin, S.K. A review of alkaline solid polymer membrane in the application of AEM electrolyzer: Materials and characterization. Int J Energy Res. 2021; 45(13): 18337–18354. https://doi.org/10.1002/er.6983
- 16. Barnes A.M., Liu B., Buratto S.K. Humidity-dependent surface structure and hydroxide conductance of a model quaternary ammonium anion exchange membrane. Langmuir. 2019; 35(44): 14188–14193. https://doi.org/10.1021/acs.langmuir.9b02160
- 17. Wijaya G.H.A., Im K.S., Nam S.Y. Advancements in commercial anion exchange membranes: A review of membrane properties in water electrolysis applications. Desalin. Water Treat. 2024; 320: 100605. https://doi.org/10.1016/j.dwt.2024.100605
- Khalid H., Najibah M., Park H.S., Bae C., Henkensmeier D. Properties of anion exchange membranes with a focus on water electrolysis. Membranes. 2022; 12(10), 989. https://doi.org/10.3390/ membranes12100989
- Giovanelli A., Pozio A., Pucci A., Geppi M., Martini F. Fumasep FAA-3-PK-130: Exploiting multinuclear solid-state NMR to shed light on undisclosed structural properties. Polymer. 2024; 311: 127536. https://doi.org/10.1016/j.polymer.2024.127536
- Hyun J., Kim H. Powering the hydrogen future: current status and challenges of anion exchange membrane fuel cells. Energy Environ. Sci. 2023; 16(12): 5633–5662. https://doi.org/10.1039/D3EE01768K
- 21. Endrődi B., Kecsenovity E., Samu A., Halmágyi T., Rojas-Carbonell S., Wang L., Yan Y., Janáky C. High carbonate ion conductance of a robust Piper-ION membrane allows industrial current density and conversion in a zero-gap carbon dioxide electrolyzer cell. Energy Environ. Sci. 2020; 13(11): 4098–4105. https://doi.org/10.1039/D0EE02589E
- 22. Rutjens B., von Foerster K., Schmid B., Weinrich H., Sanz S., Tempel H., Eichel R. Impact of the PiperION anion exchange membrane thickness on the performance of a CO₂-to-HCOOH three-compartment electrolyzer. Ind. Eng. Chem. Res.

- 2024; 63(9): 3986–3996. https://doi.org/10.1021/acs.iecr.3c04459
- 23. Domańska A., Skitał P. Electrodeposition of alloy nanostructures (Co-Ni) in the presence of sodium benzene sulfonate (SBS) and their application in alkaline hydrogen evolution. Molecules. 2025; 30(8): 1771. https://doi.org/10.3390/molecules30081771
- 24. Pan D., Bakvand P.M., Pham T.H., Jannasch P. Improving poly(arylene piperidinium) anion exchange membranes by monomer design. J. Mater. Chem. A. 2022; 10: 16478–16489. https://doi.org/10.1039/D2TA03862E
- 25. Li X., Zhao L., Yu J., Liu X., Zhang X., Liu H., Zhou W. Water splitting: From Electrode to green energy system. Nano-Micro Lett. 2020; 12: 131. https://doi.org/10.1007/s40820-020-00469-3
- 26. Darband G.B., Aliofkhazraei M., Shanmugam S. Recent advances in methods and technologies for enhancing bubble detachment during electrochemical water splitting. Renewable Sustainable Energy Rev. 2019; 114: 109300. https://doi.org/10.1016/j. rser.2019.109300
- 27. Yuzer B., Selcuk H., Chehade G., Demir M.E., Dincer. Evaluation of hydrogen production via electrolysis with ion exchange membranes. Energy. 2020; 190: 116420. https://doi.org/10.1016/j.energy.2019.116420
- Wang R., Ohashi M., Ishida M., Ito H. Water transport analysis during cathode dry operation of anion exchange membrane water electrolysis. Int. J. Hydrogen Energy. 2022; 47(97): 40835–40848. https://doi.org/10.1016/j.ijhydene.2022.09.181
- 29. Tricker A.W., Lee J.K., Shin J.R., Danilovic N., Weber A.Z., Peng X. Design and operating principles for high-performing anion exchange membrane water electrolyzers. J. Power Sources. 2023; 567: 232967. https://doi.org/10.1016/j.jpowsour.2023.232967
- 30. Li D., Matanovic I., Lee A.S., Park E.J., Fujimoto C., Chung H.T., Kim Y.S. Phenyl Oxidation Impacts the Durability of Alkaline Membrane Water Electrolyzer. ACS Appl. Mater. Interfaces. 2019; 11(10): 9696–9701. https://doi.org/10.1021/ acsami.9b00711
- 31. Faid A.Y., Xie L., Barnett A.O., Seland F., Kirk D., Sunde S. Effect of anion exchange ionomer content on electrode performance in AEM

- water electrolysis. Int. J. Hydrogen Energy. 2020; 45(53): 28272–28284. https://doi.org/10.1016/j.ijhydene.2020.07.202
- 32. Kong T.H., Thangavel P., Shin S., Kwon S., Choi H., Lee H., Park N., Woo J.-J., Kwon Y. In-situ ionomerfree catalyst-coated membranes for anion exchange membrane water electrolyzers. ACS Energy Lett. 2023; 8(11): 4666–4673. https://doi.org/10.1021/acsenergylett.3c01418
- 33. Caielli T., Ferrari A.R., Bonizzoni S., Sediva E., Caprì A., Santoro M., Gatto I., Baglio V., Mustarelli P. Synthesis, characterization and water electrolyzer cell tests of poly(biphenyl piperidinium) Anion exchange membranes. J. Power Sources. 2023; 557: 232532. https://doi.org/10.1016/j.jpowsour.2022.232532
- 34. Cooper K. Characterizing through-plane and inplane ionic conductivity of polymer electrolyte membranes. ECS Trans. 2011; 41: 1371–1380. https://doi.org/10.1149/1.3635668
- 35. Lin X., Kirk D.W. An improved hydroxide conversion process of anionic exchange membranes for alkaline fuel cells. J. New Mater. Electrochem. Syst. 2019; 22(4): 173–178. https://doi.org/10.14447/jnmes.v22i4.a01
- 36. Henkensmeier D., Najibah M., Harms C., Žitka J., Hnát J., Bouzek K. Overview: state-of-the art commercial membranes for anion exchange membrane water electrolysis. J. Electrochem. En. Conv. Stor. 2021; 18(2): 024001. https://doi.org/10.1115/1.4047963
- 37. Rakhshani S., Araneo R., Pucci A., Rinaldi A., Giuliani C., Pozio A. Synthesis and characterization of a composite anion exchange membrane for water electrolyzers (AEMWE). Membranes. 2023; 13(1) 109. https://doi.org/10.3390/membranes13010109
- 38. Luo X., Rojas Carbonell S., Yan Y., Kusogil A. Structure-transport relationships of poly(aryl piperidinium) anion-exchange membranes: Eeffect of anions and hydration. J. Membr. Sci. 2020; 598: 117680. https://doi.org/10.1016/j.memsci.2019.117680
- 39. Kim Y.S. and Pivovar B.S. Moving beyond mass-based parameters for conductivity analysis of sulfonated polymers. Annu. Rev. Chem. Biomol. Eng. 2010; 1(1): 123–148. https://doi.org/10.1146/annurev-chembioeng-073009-101309